RESEARCH ARTICLE

The role of 4-hydroxyphenylpyruvate dioxygenase in enhancement of solid-phase electron transfer by *Shewanella oneidensis* MR-1

Charles E. Turick[1], Alex S. Beliaev[2], Brian A. Zakrajsek[2], Catherine L. Reardon[2], Daniel A. Lowy[3], Tara E. Poppy[4], Andrea Maloney[5] & Amy A. Ekechukwu[1]

[1]Savannah River National Laboratory, Environmental Science and Biotechnology Department, Aiken, SC, USA; [2]Pacific Northwest National Laboratory, Richland, WA, USA; [3]Nova Research Inc., Alexandria, VA, USA; [4]University of South Carolina, Aiken, SC, USA; and [5]Winthrop University, Rock Hill, SC, USA

Correspondence: Charles E. Turick, Savannah River National Laboratory, Environmental Science and Biotechnology Department, Building 999W, Aiken, SC 29808, USA. Tel.: +1 803 819 8407; fax: +1 803 819 8432; e-mail: charles.turick@srnl.doe.gov

Present addresses: Tara E. Poppy, Department of Veterinary Medicine, University of Tennessee, Knoxville, TN, USA. Andrea Maloney, South Carolina Department of Health and Environmental Control, Columbia, SC, USA.

Received 22 December 2008; revised 12 February 2009; accepted 17 February 2009. First published online 18 March 2009.

DOI:10.1111/j.1574-6941.2009.00670.x

Editor: Alfons Stams

Keywords
dissimilatory metal-reducing bacteria; pyomelanin; electron shuttle; microbial electron transfer; hydrous ferric oxide; iron minerals.

Abstract

We hypothesized that *Shewanella oneidensis* MR-1, a model dissimilatory metal-reducing bacterium, could utilize environmentally relevant concentrations of tyrosine to produce pyomelanin for enhanced Fe(III) oxide reduction. Because homogentisate is an intermediate of the tyrosine degradation pathway, and a precursor of a redox-cycling metabolite, pyomelanin, we evaluated the process of homogentisate production by *S. oneidensis* MR-1, in order to identify the key steps involved in pyomelanin production. We determined that two enzymes involved in this pathway, 4-hydroxyphenylpyruvate dioxygenase and homogentisate 1,2-dioxygenase are responsible for homogentisate production and oxidation, respectively. We used genetic analysis and physiological characterization of MR-1 strains either deficient in or displaying substantially increased pyomelanin production. The relative significance imparted by pyomelanin on solid-phase electron transfer was also addressed using electrochemical techniques, which allowed us to extend the genetic and physiological findings to biogeochemical cycling of metals. Based on our findings, environmental production of pyomelanin from available organic precursors could contribute to the survival of *S. oneidensis* MR-1 when dissolved oxygen concentrations become low, by providing an increased capacity for solid-phase metal reduction. This study demonstrates the role of organic precursors and their concentrations in pyomelanin production, solid phase metal reduction and biogeochemical cycling of iron.

Introduction

Melanin pigments are common to microorganisms and provide numerous growth and survival advantages. For instance, melanin confers protection from light in *Legionella pneumophila* (Steinert *et al.*, 1995), decreases oxidative stress in *Burkholderia cepacia* (Zughaier *et al.*, 1999) and enhances growth of *Cryptococcus neoformans* in ionizing radiation fields (Dadachova *et al.*, 2007). Melanin is used as a terminal electron acceptor, and was found to enhance dissimilatory Fe(III) oxide reduction by *Shewanella algae* BrY (Turick *et al.*, 2002, 2003), as well as reduction-linked Fe(II) chelation in *L. pneumophila* (Chatfield & Cianciotto, 2007). Microbial melanin also complexes uranium (McLean *et al.*, 1998), and, hence, may contribute to *in situ* uranium immobilization by enhancing uranium sorption to minerals (Turick *et al.*, 2008b). Given the utility of this common metabolite to microbial growth and survival, it is important to understand the environmental conditions that contribute to melanin production and, in turn, to understand the physiological advantages of melanin production.

There are several different types of melanin pigments produced by microorganisms (Prota, 1992). One particular type of melanin, pyomelanin, originates from the conversion of tyrosine and/or phenylalanine as part of the fumarate pathway (Lehninger, 1975), and is found in numerous bacterial genera (Yabuuchi & Omyama, 1972; Kotob *et al.*, 1995; Ruzafa *et al.*, 1995; David *et al.*, 1996; Sanchez-Amat

et al., 1998), including *Shewanella* (Fuqua & Weiner, 1993; Coon *et al.*, 1994; Ruzafa *et al.*, 1994; Turick *et al.*, 2002, 2008a), *Legionella* (Chatfield & Cianciotto, 2007) and *Burkholderia* (Zughaier *et al.*, 1999). Complete breakdown of these amino acids to acetoacetate and fumarate requires the activities of 4-hydroxyphenylpyruvate dioxygenase (4-HPPD) and homogentisate oxidase (Fuqua & Weiner, 1993; David *et al.*, 1996). In the absence of the latter, homogentisate is overproduced, and excreted from the cell (Coon *et al.*, 1994). Subsequent auto-oxidation and self-polymerization of homogentisate yields pyomelanin, a polyaromatic heteropolymer, which consists of numerous quinone moieties (Ruzafa *et al.*, 1995). Interestingly, homogentisate auto-oxidation occurs under declining oxygen concentrations (Ruzafa *et al.*, 1995), commonly found in the oxic-to-anoxic interface of redox-stratified environments such as tidal zones and biofilms. Microbial production of pyomelanin has been demonstrated *in situ*, in surface soils, and affects metal immobilization down to 50 cm (Turick *et al.*, 2008b).

Previous studies demonstrated that *in vivo* and *in situ* production of melanin in *Shewanella* is directly related to the presence of tyrosine and phenylalanine (Turick *et al.*, 2002, 2003, 2008a). Earlier studies have also shown that concentrations of tyrosine and phenylalanine vary considerably, from 10 to 632 mg kg^{-1}, in different types of soils (Martens & Loeffelmann, 2003; McLain & Martens, 2005). Because minute quantities (fg per cell) of pyomelanin are needed per cell to increase electron transfer (ET) rates (Turick *et al.*, 2002), the environmental concentrations of tyrosine and phenylalanine should be sufficient to accelerate pyomelanin-dependent metal reduction rates in the subsurface. We hypothesized that *Shewanella oneidensis* MR-1, a model dissimilatory metal-reducing bacterium, could utilize exogenous tyrosine to produce pyomelanin for enhanced Fe(III) oxide reduction. In this study, we elucidated the process of homogentisate production by *S. oneidensis* MR-1, and identified the key steps involved in the accumulation of pyomelanin. To better understand the environmental relevance of this redox-shuttling metabolite, we used genetic analysis and physiological characterization of MR-1 strains either deficient in or displaying substantially increased pyomelanin production. The relative significance imparted by pyomelanin on solid-phase ET was also addressed using an approach based on cyclic voltammetry (CV), which allowed us to extend the genetic and physiological findings to biogeochemical cycling of metals.

Materials and methods

Growth conditions

Shewanella oneidensis MR-1 wild-type and mutant strains were routinely maintained on tryptic soy agar. Tryptic soy broth (TSB) and a lactate (70 mM) basal salts medium (LBSM) (Turick *et al.*, 2002) with or without 300 mg L^{-1} of tyrosine were used for pyomelanin studies. Tyrosine concentrations of LBSM were based on that of TSB (McCuen, 1988). The *S. oneidensis* MR-1 cultures were grown in 25-mL aliquots aerobically at 25 °C on a rotary shaker (100 r.p.m.) for 48–72 h, unless specified otherwise. To determine whether pyomelanin production occurred without supplemental tyrosine, cultures were grown in LBSM for 48 and 240 h under the conditions described above. For electrochemical studies, cultures were grown in TSB for 72 h. To determine the effect of surface-associated pyomelanin on ET, sterile (autoclaved) pyomelanin (0.1 mg mL^{-1}) was added to cultures of the pyomelanin-deficient strain (Δ*melA*) after 24 h of growth. Pyomelanin production under anaerobic conditions was determined in LSBM with 30 mM fumarate as the terminal electron acceptor and 1 mg mL^{-1} tyrosine with oxygen-free N_2 as the head-space gas in viton capped test tubes. Following 72 and 150 h of incubation at 25 °C, the liquid was analyzed aerobically and anaerobically for pigment production by spectrophotometry ($A_{400\,nm}$).

Growth studies were conducted as described above using basal salts medium supplemented with 5 mM tyrosine as the sole carbon source. For anaerobic growth, 30 mM fumarate served as the terminal electron acceptor with O_2-free N_2 as the head space gas. Cell density was determined spectrophotometrically ($OD_{600\,nm}$).

Pigment characterization

The production of melanin precursors by *S. oneidensis* MR-1, 3,4-dihydroxy-phenylalanine (DOPA) (Prota, 1992) and/or homogentisate was measured in cell-free supernatants of tyrosine-supplemented (300 mg L^{-1}) LBSM-grown cultures, using high-pressure capillary electrophoresis (HPCE) with a Celect H150 C-8 bonded phase capillary column. To prevent oxidation of precursors to melanin pigments, DOPA and homogentisate standards were dissolved in 4 mM ascorbate to a final concentration of 4 mM each. Homogentisate and DOPA were also determined by colorimetric methods. DOPA analysis consisted of the DOPA nitration method (Waite & Benedict, 1984). Homogentisate content was measured based on its reaction with cysteine to form 1,4-thiazine, according to the previously described methods (Fellman *et al.*, 1972).

Characterization of cell-free supernatants for humic- and melanin-type properties was performed as described elsewhere (Ellis & Griffiths, 1974; Turick *et al.*, 2002). Soluble pyomelanin was quantified spectrophotometrically ($A_{400\,nm}$), as described previously (Turick *et al.*, 2003). This technique incorporated known concentrations of concentrated bacterial pyomelanin and pure pyomelanin produced by the auto-oxidation of homogentisate, which served as

quantitative standards. Determination of pigment production from 4-hydroxyphenylpyruvate was performed in BSM with 5 mM 4-hydroxyphenylpyruvate. Cell-free supernatants of *S. oneidensis* MR-1 wild-type and mutant cultures pregrown for 48 h at 25 °C were analyzed spectrophotometrically ($A_{400\,nm}$) for pigment production. Cell-associated pyomelanin was quantified as described previously (Turick *et al.*, 2003) with slight modification to incorporate the nitro blue tetrazolium assay (Paz *et al.*, 1991) with a detection limit of 0.5 μg mL^{-1}. Results of this assay compared well with those obtained by the spectroscopic analysis ($OD_{400\,nm}$) of cell suspensions, which was used throughout the study. The methods included a known cell density of pyomelanin-producing cells blanked against an equal cell density of the pyomelanin-deficient strain (Δ*melA*). Pyomelanin was quantified as described above, and calculated per cell. Cell density was determined after acridine orange staining, with an epifluorescence microscope (Hobbie *et al.*, 1977).

Inhibition of pyomelanin production

Sulcotrione [2-(2-chloro-4-methane sulfonylbenzoyl)-1, 3-cyclohexanedione] (Zeneca Ag. Products, Richmond, CA) is a potent inhibitor of 4-HPPD (Schulz *et al.*, 1993; Secor, 1994; Lee *et al.*, 1997). *Shewanella oneidensis* MR-1 was grown for 48 h in tyrosine-supplemented (300 mg L^{-1}) LBSM or TSB with 18 μM sulcotrione to test its effects on pyomelanin production. Sulcotrione was added continuously with a syringe pump to maintain an 18 μM concentration.

Construction and complementation of *melA* and *hmgA* mutants of *S. oneidensis* MR-1

In-frame deletion mutagenesis was performed using the method originally described by Link *et al.* (1997), with minor modifications. Upstream and downstream fragments flanking the target locus were PCR amplified using *S. oneidensis* MR-1 genomic DNA, and fused via overlap extension PCR (Ho *et al.*, 1989). The fusion PCR amplicon was ligated into XcmI-digested pDS3.1 (Wan *et al.*, 2004). The resulting recombinant plasmids were used to transform *Escherichia coli* β-2155 (Dehio & Meyer, 1997) or WM3064 (Saltikov *et al.*, 2003), and subsequently transferred to *S. oneidensis* MR-1 by conjugation. The primary integrants were selected by plating on Luria–Bertani medium containing 7.5 μg mL^{-1} gentamycin. Selection for a second homologous recombination to remove the plasmid sequence was accomplished by sucrose counter-selection (Blomfield *et al.*, 1991). Sucrose-resistant colonies were screened for sensitivity to gentamycin and then screened for deletion of the gene of interest using PCR. The resulting PCR amplicon was then used as the template for DNA sequencing of the deleted and flanking regions involved in the recombination events (ACGT Inc., Wheeling, IL).

Δ*melA* and Δ*hmgA* were complemented with wild-type copies of the deleted gene cloned into the broad-host-range-vector pBBR1MCS-5 (de Lorenzo *et al.*, 1990). Briefly, *melA* and *hmgA* were PCR-amplified from purified MR-1 DNA with Phusion High-Fidelity DNA Polymerase (Finnzymes, Finland) using the following sets of primers: *melA*F (5′-GAATTAATCAAGAGGAACAG-3′) and *melA*R (5′-CTTACAGTACGCCGCGGC-3′); *hmgA*F (5′-CGCA TAAAACTCAAGGATCC-3′) and *hmgA*R (5′-CTGCCAA TCGCTGTGTTAG-3′). The amplified fragments were ligated into the SmaI (New England Biolab, Beverly, MA) site of pBBR1MCS-5 and subsequently transferred into the respective deletion mutants via conjugation according to a published protocol (de Lorenzo *et al.*, 1990). The plasmids were sequenced using M13F and M13R primers to verify the correct orientation and sequence (Agencourt, Beverly, MA).

Quantification of ET

Hydrous ferric oxide (HFO) (50 mM) was used to measure Fe(III) reduction kinetics in carbonate buffer with H_2 or lactate as the electron donor, according to a previously described methodology (Turick *et al.*, 2002, 2003). To determine the effect of melanin on HFO reduction, an autoclaved pyomelanin solution (1 μg mL^{-1} final concentration) was spiked into selected suspensions of the Δ*melA* mutant. For determining Fe(III) oxide reduction activity with lactate (70 mM) as the electron donor, cells were pregrown in TSB and washed as above, except that they were resuspended in LBSM with HFO and monitored over time for Fe(II) production. Cell densities in these studies were normalized to 10^8 cells mL^{-1} with H_2 as the electron donor and 10^7 cells mL^{-1} with lactate as the electron donor, as determined with acridine orange staining and epifluorescence microscopy (Hobbie *et al.*, 1977). Fe(II) was measured spectrophotometrically using the ferrozine assay as described elsewhere (Turick *et al.*, 2002).

In order to more precisely characterize the role of pyomelanin as a surface-associated electron shuttle, electrochemical studies were designed for whole bacterial cells. CV can provide valuable information on ET, which proceeds in biological systems. With CV, a controlled electric potential is applied to the working electrode and the current is recorded. When the potential is swept in the positive direction, it drives the oxidation reaction, and when the scan is reversed, reduction is favored. Our studies incorporated concentrated suspensions (10 ×) of whole bacterial cells under anaerobic conditions. Operational conditions included washed (3 ×) cell suspensions of cultures grown aerobically in TSB. Cultures were resuspended in phosphate-buffered saline (PBS) for electrochemical studies. Before electrochemical

analyses, the cell suspensions were made anaerobic by purging continuously with O_2-free N_2 gas for 15 min. Electrochemical measurements were performed in the three-electrode geometry with a carbon paste working electrode, a Pt counter electrode (Bioanalytical Systems, BAS, West Lafayette, IN) and an Ag/AgCl, 3 M KCl reference (BAS), all immersed in the anaerobic cell suspension that was blanketed with nitrogen gas throughout the studies. Potentials measured relative to Ag/AgCl, 3 M KCl reference can be converted to values relative to the standard hydrogen electrode (SHE), according to the following equation (Bard *et al.*, 1985):

$$E_{\mathrm{SHE}}[\mathrm{V\ vs.\ SHE}] = E_{\mathrm{Ag(RE)}}[\mathrm{V\ vs.\ Ag(RE)}] - 0.23695 + 4.8564 \times 10^{-4} t,$$

where t is temperature in °C, and the second- and third-order terms are neglected. Potential sweep originated in the positive direction at a scan rate of 850 mV s^{-1} for all CVs in this study, using a model 100B/A potentiostat (BAS). This sweep rate was chosen to allow for rapid analyses in order to prevent physiological changes in the cultures throughout the investigation. Sweep rates from 100 to 1700 mV s^{-1} were analyzed and no significant peak distortions were detected at 850 mV s^{-1} (data not shown).

A total of six sweeps were performed with each culture. Duplicate CV values derived from each measurement were averaged and the fifth and sixth averaged sweeps were reported here. Between each set of measurements using different cultures, the working electrodes were rinsed in deionized water (DIW), followed by a methanol rinse, and sonication for 10 min in DIW. For each strain analyzed, a CV of the washed bare electrode in PBS was recorded, which served as a no-cell control for the next series of voltammetry studies. In addition, cell-free liquid from each cell suspension was analyzed (as described above) for electrochemical activity in the bulk phase. Formal potentials ($E^{\circ\prime}$) from CVs were calculated as the mean value of oxidation and reduction peak potentials. Apparent rate constant values (k° values) were derived according to Laviron's theory (Laviron, 1983; Finklea, 2001), from peak-to-peak potential separation, by assuming a one-ET mechanism. Simulation of the CVs was performed by means of the software provided for the Model 660a Electrochemical Workstation by CH Instruments (Austin, TX).

The contribution of pyomelanin to the electrochemical activity was further determined by subtracting the CVs of Δ*melA* from those of *S. oneidensis* MR-1 and Δ*melA* supplemented with autoclaved pyomelanin. This approach provided for increased detail of surface electrochemical behavior. The effect of pyomelanin concentrations on ET rates was determined by mixing powdered, sterile pyomelanin with carbon paste at ratios of 10 : 90 and 20 : 80 pyomelanin to carbon paste (Serpentini *et al.*, 2000). CVs were produced as above and compared with those of bacterial suspensions.

Riboflavin analyses

Riboflavin (2 and 4 μM) with and without 100 μg mL^{-1} of autoclaved pyomelanin in pH 7.12 PBS was analyzed with linear sweep stripping voltammetry (LSSV) in order to identify one of the peaks from CV studies. Riboflavin and riboflavin/pyomelanin mixtures were stored at 25 °C for 4 h before analyses. The reference and counter electrodes were Ag/AgCl and Pt, respectively. The glassy carbon working electrode (BAS) was polished with aluminum oxide, rinsed in DIW and sonicated for 10 min before each use. Deposition time in all LSSV studies was 10 s at −800 mV (vs. Ag/AgCl) followed by a scan rate of 100 mV s^{-1} from −800 to 0 mV.

Adsorption studies

To determine whether riboflavin complexed with pyomelanin, 4 μM riboflavin was combined with 0, 100, 200, 400 and 800 μg mL^{-1} sterile pyomelanin. After the mixtures were shaken at 100 r.p.m. for 20 h at 25 °C, pyomelanin was physically separated from riboflavin through centrifugal dialysis (Turick *et al.*, 2008b) (5-kDa MW cut-off) and the pyomelanin-free liquid was quantified spectrophotometrically ($A_{445\ nm}$).

Results

Characterization of melanin production

Growth of *S. oneidensis* MR-1 on tyrosine-supplemented LBSM resulted in the production of a reddish-brown pigment during late log and early stationary phases during aerobic incubation but not under anaerobic conditions. During aerobic incubation, dissolved oxygen concentrations dropped from 108 nM mL^{-1} (just before inoculation) to 1.74(±0.085) nM mL^{-1}. At pH ≤ 2, the soluble cell-free pigment precipitated rapidly displaying melanin and humic-like properties (Ellis & Griffiths, 1974). Following precipitation, washing and dialysis, the dried (60 °C) pigment produced black powder with the following melanin-like characteristics (Ellis & Griffiths, 1974): insolubility in organic solvents (ethanol, chloroform and acetone); solubility in NaOH solutions at pH ≥ 10; decolorization in H_2O_2; precipitation by $FeCl_3$; and inability to filter through 8-kDa dialysis membrane.

HPCE analysis of cell-free supernatants from tyrosine-supplemented LBSM cultures identified a peak that coeluted with the homogentisic acid (HGA) standard (retention time, 2.69 min), indicating production of homogentisate,

the precursor of pyomelanin. In contrast, DOPA (retention time, 2.42 min), the precursor of eumelanin, was not detected. These data specifically implied that the production of pyomelanin in MR-1 is dependent on the function of 4-HPPD, which is responsible for homogentisate production in the tyrosine catabolic pathway.

To confirm the role of 4-HPPD in pyomelanin production, *S. oneidensis* MR-1 cultures were grown in TSB and tyrosine-supplemented LBSM media for 48 h, in the presence or the absence of sulcotrione, a competitive inhibitor of 4-HPPD. Cultures grown in LBSM with both sulcotrione and tyrosine had no pigmentation relative to cultures without tyrosine (Table 1). Decreased pyomelanin production in cell-free supernatants from TSB-grown cultures was also evident in sulcotrione-treated cultures. Similarly, after 48 h of growth in LBSM with sulcotrione and no tyrosine, no pigmentation was detected (Table 1), suggesting that sulcotrione specifically inhibits 4-HPPD-dependent conversion of tyrosine to pyomelanin. To ensure that the inhibitor did not exert any effect on the growth of *S. oneidensis* MR-1, we measured turbidities ($OD_{600\,nm}$) of cultures grown in the presence and absence of sulcotrione. Cell densities mL^{-1} from TSB ($1.6 \times 10^8 \pm 3.5 \times 10^7$) were similar to those from TSB+sulcotrione ($1.5 \times 10^8 \pm 3.4 \times 10^7$) and cell densities mL^{-1} from LBSM ($4.4 \times 10^7 \pm 2.6 \times 10^6$) were similar to those from LBSM+sulcotrione ($4.4 \times 10^7 \pm 5.1 \times 10^7$).

Genetic analysis of melanin production in *S. oneidensis* MR-1

The genome sequence suggests the presence of a complete tyrosine degradation pathway in *S. oneidensis* MR-1, and its components are identified in the KEGG database (http://www.kegg.com). Although no obvious homologs of tyrosinase or laccase were identified in the genome of MR-1 (http://www.tigr.org), a putative *melA* (SO1962) gene encoding 4-HPPD was present. *melA* is located 120 base pairs downstream of an ORF, encoding a conserved hypothetical protein (SO1963). To identify the potential function of SO1963, we conducted protein–protein BLAST search across the NCBI nonredundant database. Results of the search indicated that SO1963 is 45% identical and 61% similar to the putative homogentisate 1,2-dioxygenase (HGD) from *Bacillus anthracis* strain Ames and 23% identical and 42% similar to the human HGD. In many organisms, HGD is a part of the tyrosine catabolic pathway, and is involved in the oxidation of homogentisate to acetoacetate, which is subsequently assimilated through the tricarboxylic acid cycle. To reflect the sequence similarity and the potential function of SO1963 in *S. oneidensis* MR-1, the identified gene was designated as *hmgA*.

To elucidate the functions of SO1962 and SO1963 in melanin production, we generated in-frame deletion mutants lacking putative *melA* and *hmgA* genes. The resulting mutants, Δ*melA* and Δ*hmgA*, were tested for the production of pyomelanin during growth on tyrosine-supplemented LBSM and TSB media. While pyomelanin production was completely abolished in the Δ*melA* mutant, Δ*hmgA* strain deficient in the putative HGD displayed substantial overproduction of this electron-shuttling compound relative to the wild-type *S. oneidensis* MR-1 (Table 1). Aerobic growth with tyrosine as the sole carbon source was displayed by the wild-type MR-1 but not by Δ*melA* or Δ*hmgA*. Both wild type and Δ*hmgA* produced pigment from 4-hydroxyphenylpyruvate, whereas Δ*melA* did not. Interestingly, the overproduction of pyomelanin by Δ*hmgA* was notable in the stationary phase, when the Δ*hmgA* strain was grown on minimal medium without the addition of tyrosine, exceeding the wild-type production levels by five- to eightfold (Table 1). Following complementation, pyomelanin production was restored in the Δ*melA* mutant, while the complemented Δ*hmgA* strain no longer overproduced pyomelanin.

Pyomelanin enhancement of Fe(III) oxide reduction

Anaerobic resting-cell studies using H_2 as the electron donor were conducted to quantify the role of 4-HPPD on

Table 1. Production of pyomelanin by wild-type and mutant strains of *Shewanella oneidensis* MR-1

	Soluble pyomelanin ($mg\,mL^{-1}$)				Cell-associated pyomelanin (fg per cell)			HFO reduced* [μM Fe(II)]
Strain	TSB	LBSM+300 $mg\,L^{-1}$ tyrosine (48 h)	LBSM (48 h)	LBSM (240 h)	TSB	LBSM+300 $mg\,L^{-1}$ tyrosine (48 h)	LBSM no tyrosine (240 h)	LBSM no tyrosine (240 h)
MR-1	0.427 (0.046)	0.270 (0.025)	ND	0.032 (0.009)	66.32 (4.63)	36.50 (4.60)	4.14 (0.964)	12.9 (0.21)
MR-1+sulcotrione	ND	ND	ND	NI	NI	NI	NI	NI
Δ*melA*	ND	ND	ND	ND	ND	ND	ND	9.8 (0.96)
Δ*hmgA*	0.987 (0.167)	0.680 (0.074)	ND	0.162 (0.003)	153.40 (16.87)	86.44 (16.70)	37.07 (3.214)	16.6 (0.32)

*Data from resting cell studies of cells pregrown in LBSM without tyrosine.
SDs in parentheses.
ND, not detected; NI, not included in assay.

pyomelanin production and HFO reduction rates in *S. oneidensis* MR-1. TSB-grown cells with sulcotrione (nonmelanized) had a diminished capacity for HFO reduction, when compared with cells grown on TSB in the absence of sulcotrione (Fig. 1a). Similarly, with LBSM-grown cultures, only those supplemented with tyrosine but without sulcotrione (melanized cells) demonstrated enhanced HFO reduction capacities as compared with those grown either in the absence of tyrosine or in the presence of sulcotrione (nonmelanized cells) (Fig. 1b).

Resting-cell studies of mutant and wild-type cultures of *S. oneidensis* MR-1 grown in TSB or tyrosine-supplemented LBSM also demonstrated increased HFO reduction capacity as a function of pyomelanin production. Using H_2 as the electron donor, Δ*melA* strain displayed a diminished capacity for HFO reduction relative to the wild type, while the pyomelanin-overproducing strain (Δ*hmgA*) exceeded the HFO reduction capacity of the wild-type *S. oneidensis* MR-1 (Fig. 2a and b). Addition of exogenous pyomelanin resulted in a substantial increase in HFO reduction rates displayed by Δ*melA* (Fig. 2b). With lactate as the electron donor, Δ*melA* demonstrated a decreased ability to reduce Fe(III) oxides compared with wild type and Δ*hmgA* (Fig. 3). In contrast to H_2, no significant differences were observed in lactate-driven HFO reduction between Δ*hmgA* and wild-type cultures of *S. oneidensis* MR-1.

Electrochemical analysis of pyomelanin-mediated ET

Electrochemical studies were conducted to gain insight into the ET behavior at the cell surface relative to pyomelanin concentration. Cyclic voltammograms from concentrated whole-cell suspensions demonstrated redox activity as a function of pyomelanin content. As shown in Fig. 4, the wild-type and the two mutant strains displayed different CVs as a function of pyomelanin production or exposure to pyomelanin during growth. The wild-type strain

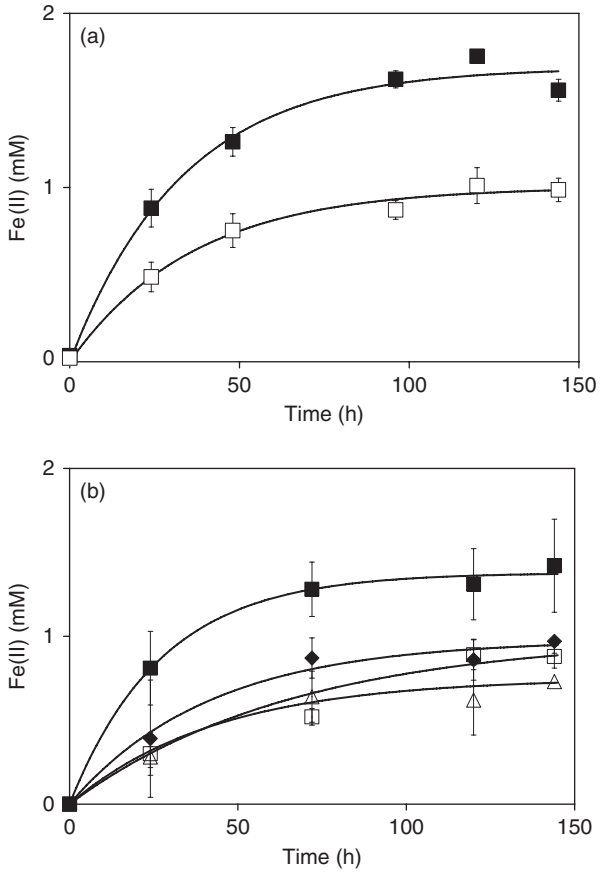

Fig. 1. Resting cell studies demonstrated inhibitory effects of sulcotrione on pyomelanin production and HFO reduction by *Shewanella oneidensis* MR-1. (a) Cells pregrown in TSB with (□) and without (■) sulcotrione. (b) Cells pregrown in LBSM (◆), LBSM and sulcotrione (△), LBSM with tyrosine (■), and LBSM with tyrosine and sulcotrione (□).

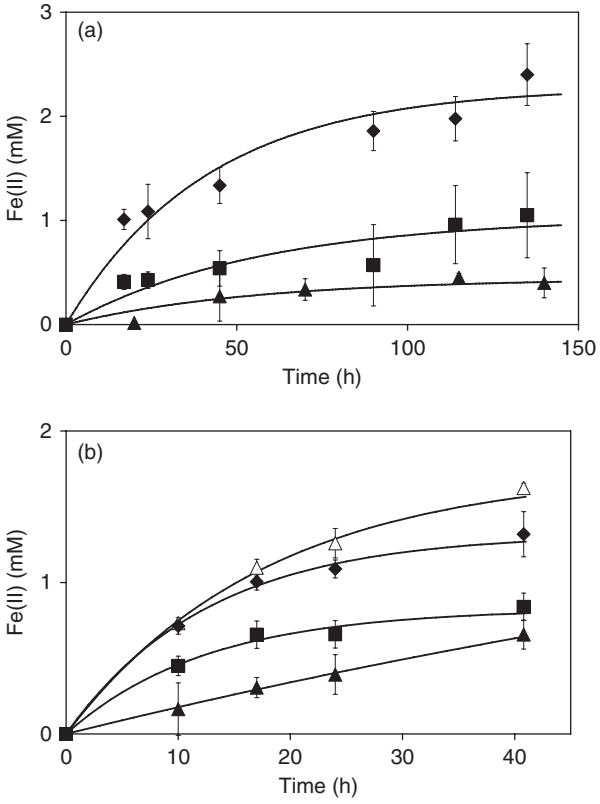

Fig. 2. HFO reduction by three strains of *Shewanella oneidensis* with H_2 as the electron donor. Resting cell studies of cells pregrown in (a) TSB and (b) LBSM + 300 mg L^{-1} tyrosine demonstrated an increased HFO reduction efficiency by the pyomelanin-overproducing strain (Δ*hmgA*) (◆) relative to MR-1 (■) and the pyomelanin-deficient mutant (Δ*melA*) (▲), which demonstrated the least amount of HFO reduction. Addition of pyomelanin (10 μg mL^{-1}) to resting cell cultures of Δ*melA* (△) pregrown in LBSM demonstrated drastically increased levels of HFO reduction.

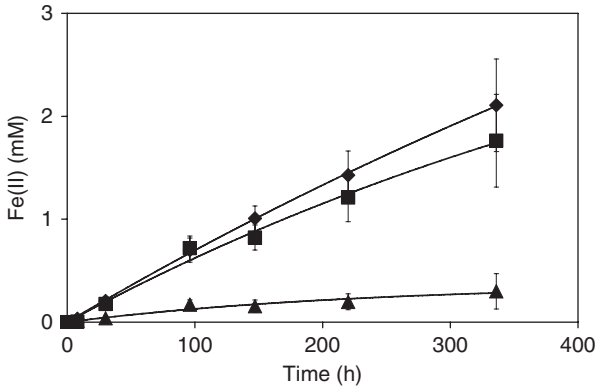

Fig. 3. HFO reduction by three strains of *Shewanella oneidensis* with lactate as the electron donor. Cells pregrown aerobically in TSB and inoculated into anaerobic LBSM demonstrated greater HFO reduction efficiency by the pyomelanin-overproducing strain (Δ*hmgA*) (◆) and MR-1(■) compared with that of the pyomelanin-deficient mutant (Δ*melA*) (▲), which demonstrated the least amount of HFO reduction.

S. oneidensis MR-1 had an $E^{\circ\prime}$ of about −485 mV vs. Ag/AgCl, 3 M KCl reference, henceforth Ag(RE) (Fig. 4a). Another slight oxidation peak was produced by the wild type around 550 mV vs. Ag(RE), but a reduction peak was not evident (Fig. 4a). In contrast, only one redox couple was detected from Δ*melA* with an $E^{\circ\prime}$ of about −566 mV vs. Ag(RE) (Fig. 4b) and the current response was diminished as compared with that of the wild type (Fig. 4a and b). Growth of Δ*melA* in the presence of 0.1 mg mL^{-1} of pyomelanin, however, resulted in an increase in the $E^{\circ\prime}$ to *c.* −474 mV vs. Ag(RE), which is similar to the values displayed by the wild type and 92 mV greater than that of Δ*melA* grown without supplemental pyomelanin (Fig. 4c). In addition, a second small oxidation peak was detected around 470 mV vs. Ag(RE), which is attributed to pyomelanin addition and its sorption to the cell surface.

Two obvious redox couples were generated in the CV of Δ*hmgA* (Fig. 4d). The formal potential of the first, near −474 mV vs. Ag(RE), was similar to that of *S. oneidensis*

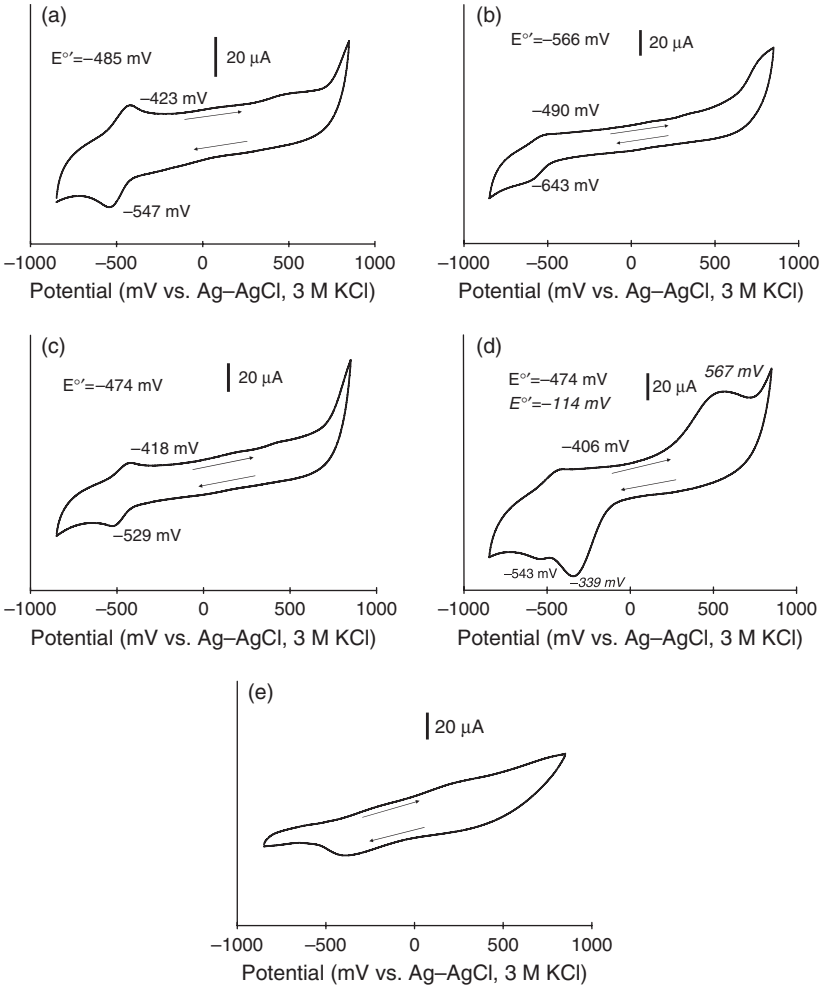

Fig. 4. CV of whole cell suspensions. Redox activity of whole cell suspensions was a function of pyomelanin content: (a) *Shewanella oneidensis* MR-1; (b) pyomelanin-deficient strain (Δ*melA*); (c) pyomelanin-deficient strain (Δ*melA*) incubated with 10 μg mL^{-1} pyomelanin; (d) pyomelanin-overproducing strain (Δ*hmgA*). Pyomelanin increased the formal potential of redox couples and increased the current response from cells. Cell-free supernatants derived from the same cultures did not produce significant electrochemical activity (e), demonstrating that the electrochemical activity was at the cell surface, rather than electron shuttles in the bulk solution. Arrows indicate sweep direction.

MR-1 wild type and the pyomelanin-exposed Δ*melA* cultures (Fig. 4a, c and d). A second redox couple, recorded at $E^{\circ\prime} = 114$ mV vs. Ag(RE), was likely due to the abundance of surface-associated pyomelanin produced by this strain. Cell-free supernatants derived from the same cultures did not produce significant electrochemical activity (Fig. 4e), demonstrating that the CVs of the cell suspensions were due to electrochemical activity at the cell surface, rather than electron shuttles in the bulk solution.

Background subtractions of CVs of Δ*melA* from those of Δ*melA* with supplemental pyomelanin and *S. oneidensis* MR-1 were conducted to gain more precise information regarding the electrochemical behavior of the cell surface, as affected by low concentrations of pyomelanin. Both strains MR-1 and Δ*melA* (with supplemental pyomelanin) revealed three redox couples with strong similarities (Fig. 5, labeled A, B and C). The redox couple labeled A is similar to that of riboflavin, a soluble electron shuttle produced by *S oneidensis* MR-1 (Marsili *et al.*, 2008). Riboflavin also demonstrates a two-electron reduction (Pereira *et al.*, 2003) as shown here (Fig. 5).

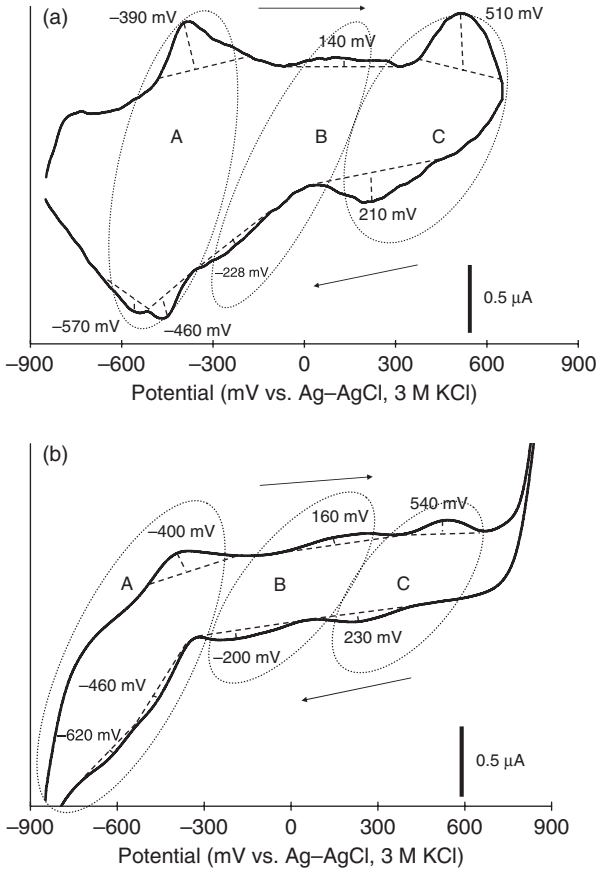

Fig. 5. Effect of pyomelanin on CV of whole cell suspensions. CVs obtained from whole cell suspensions of the pyomelanin-deficient strain (Δ*melA*) were subtracted from those of *Shewanella oneidensis* MR-1 (a) and Δ*melA*, grown with supplemental pyomelanin (b). Results revealed three redox couples designated as A, riboflavin; B, cytochrome; and C, pyomelanin. Arrows indicate sweep direction.

LSSV was used to characterize the redox couple with the lowest $E^{\circ\prime}$ described above. Riboflavin demonstrated a peak potential near -452 to -434 mM vs. Ag(RE) in the presence and the absence of pyomelanin (Fig. 6). These values are similar to riboflavin from previous electrochemical studies (Marsili *et al.*, 2008). It is noteworthy that the peak current of riboflavin at both 2 and 4 μM increased in the presence of 100 μg mL^{-1} pyomelanin, but pyomelanin alone did not demonstrate electrochemical activity in this range (Fig. 6). Riboflavin did not demonstrate complexation with pyomelanin based on adsorption studies.

The second couple (Fig. 5, label B) was unexpected but was consistent with that of cytochromes of various strains of *Shewanella* sp. described previously (Kim *et al.*, 2002). The oxidation peak of the third redox couple (Fig. 5, label C) is similar to that of Δ*hmgA* (Fig. 4d) and is ascribed to pyomelanin. To confirm this result, dried concentrated pyomelanin mixed with carbon paste was analyzed. The pyomelanin/carbon paste electrode (10 mg pyomelanin) (Fig. 7a) demonstrated redox activity with an oxidation peak similar to that of Δ*hmgA*, (Fig. 4d) but a more positive reduction peak with the resulting $E^{\circ\prime} = 253$ mV vs. Ag(RE). To determine whether pyomelanin concentration contributed to the shift in reduction peaks, 20 mg of pyomelanin combined with 80 mg carbon paste was analyzed. The higher pyomelanin concentration demonstrated a negative shift in the reduction peak (Fig. 7b), but the oxidation peak was similar to the other CVs (Figs 4d, 5 and 7a). The shift in the reduction peak from 17 to -614 mV likely resulted in a decrease in the rate of ET as a function of pyomelanin concentration as described previously with other electroactive compounds (Pereira *et al.*, 2003). This concentration-dependent shift in the reduction peak of pyomelanin (Figs 4 and 5) coincides with bacterial pyomelanin concentrations (Table 1). In all cases, the pyomelanin CVs were reproducible over five consecutive cycles, as indicated in Fig. 7a; scans exhibit continual oxidation and reduction; hence, it demonstrates the electron-shuttling capacity of pyomelanin.

Effect of prolonged growth on pigment production and HFO reduction

In order to determine whether pyomelanin production was possible without exogenous tyrosine, cultures were grown in LBSM in the absence of tyrosine for extended periods. Growth on LBSM did not result in any detectable pyomelanin production within the first 48 h in any of the tested strains (Table 1). HFO reduction rates displayed by resting cells from these cultures were also similar (data not shown). However, when incubation was extended to 240 h,

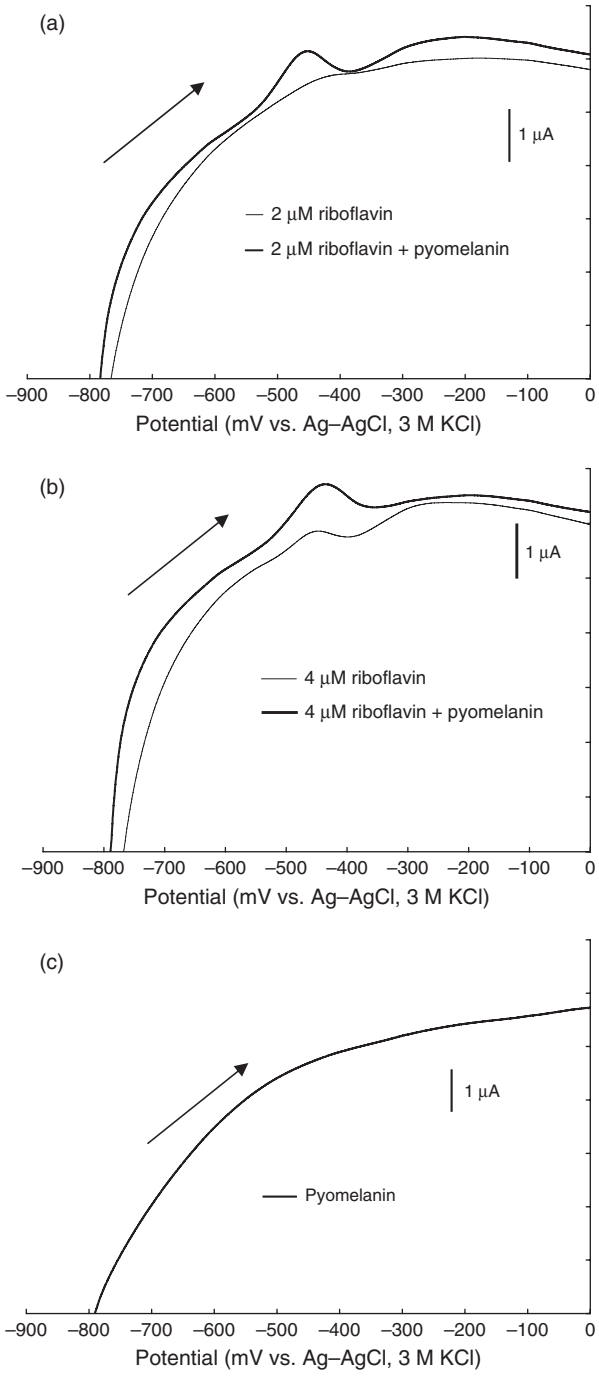

Fig. 6. Effect of pyomelanin on electrochemical behavior of riboflavin. LSSV demonstrated a peak current increase from 2 μM riboflavin (a) and 4 μM riboflavin (b) in the presence of pyomelanin (100 μg mL^{-1}) compared with riboflavin alone, after a 15-s deposition time at − 800 mV vs. Ag–AgCl, 3M KCl. The sweep rate was 50 mV s^{-1}. (c) Pyomelanin alone did not demonstrate electrochemical activity under these analytical conditions. Arrows indicate sweep direction.

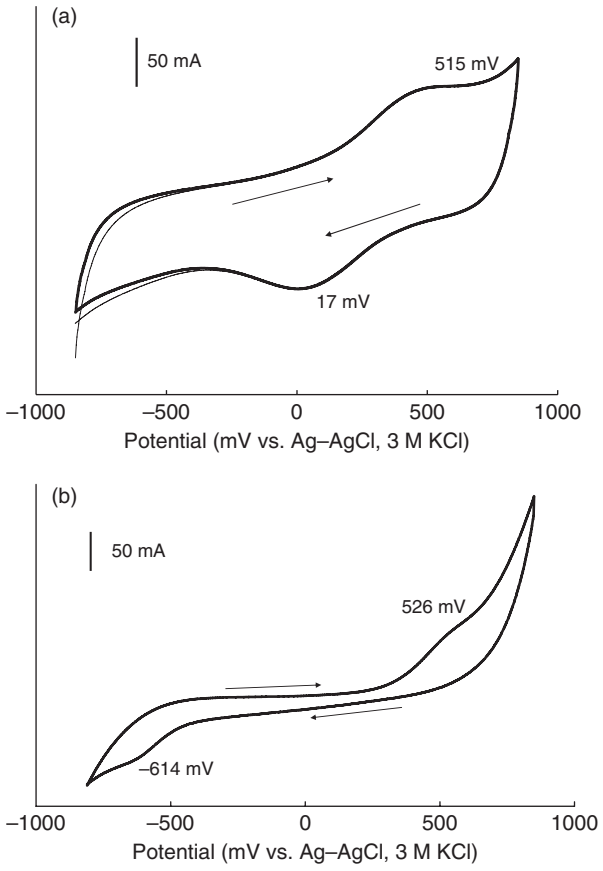

Fig. 7. CVs of dried pyomelanin incorporated into carbon paste electrodes: (a) 10 mg pyomelanin, 90 mg carbon paste and (b) 20 mg pyomelanin, 80 mg carbon paste. Scans demonstrate differences in peak separation as a function of pyomelanin concentration. Scans 1 and 2 (a) (light line) along with 5 and 6 (dark line) are reported to illustrate the reproducibility of electrochemical activity, demonstrating electron shuttling by pyomelanin. Arrows indicate sweep direction.

pyomelanin was detected in the medium supernatant and cell surfaces of Δ*hmgA* and *S. oneidensis* MR-1 (Table 1). In subsequent resting-cell studies, the Δ*hmgA* strain reduced HFO to the greatest degree, followed by *S. oneidensis* MR-1, with the least HFO reduction displayed by Δ*melA* (Table 1).

Discussion

Obligate respiration in *S. oneidensis* MR-1 requires physiological versatility during periods of declining oxygen concentrations. The presence of humic compounds and production of nano-wires or electron shuttles provides a means of accessing metal oxides as terminal electron acceptors (Lloyd, 2003; Gorby *et al.*, 2006). The utilization of melanin pigments as an electron shuttle to mineral oxides offers a potential means of enhanced survival during periods of declining oxygen concentrations. The probability of this

would depend on the environmental availability of melanin precursors and the resulting energetic advantage resulting from melanin production.

In this study, we demonstrated that *S. oneidensis* MR-1 utilizes tyrosine under low oxygen concentrations to produce homogentisate via a 4-HPPD-dependent pathway. 4-HPPD requires oxygen (Lindblad *et al.*, 1977) and, hence, pigmentation did not occur under anaerobic conditions with fumarate as the terminal electron acceptor. Because Fe(II) inhibits 4-HPPD and pyomelanin production (Lindblad *et al.*, 1977; Turick *et al.*, 2008a, b), Fe(III) was not used as a terminal electron acceptor. The resultant pigment, pyomelanin, is also produced by *Shewanella collwelliana* (Fuqua & Weiner, 1993; Ruzafa *et al.*, 1994) and *S. algae* BrY (Turick *et al.*, 2002, 2003). The absence of HGD or its decreased activity relative to 4-HPPD results in the overproduction of homogentisate, ultimately leading to extracellular pyomelanin formation. Several lines of evidence were used to confirm the metabolic pathway involved in pyomelanin production in *S. oneidensis* MR-1: pigment production was inhibited by (1) the 4-HPPD inhibitor sulcotrione; (2) the absence of pyomelanin production in the Δ*melA* strain and the abundance of pyomelanin in the Δ*hmgA* strain; and (3) pigment production from 4-hydroxyphenylpyruvate by strains MR-1 and Δ*hmgA*, but not Δ*melA*. High concentrations of pyomelanin produced by Δ*hmgA* compared with the wild-type MR-1 suggested that the HGA oxidase is functional but its activity is lower than that of the upstream enzyme 4-HPPD in the wild-type strain, resulting in excess HGA production.

When pyomelanin is produced by *Shewanella*, this redox-active metabolite serves as a terminal electron acceptor and mediates ET to solid-phase metal oxides by *S. algae* BrY (Turick *et al.*, 2002, 2003). Tyrosine concentrations in both TSB and LBSM correlated with pyomelanin production and increased HFO reduction. Addition of soluble pyomelanin to resting cells of melanin-deficient Δ*melA* strain increased the rate and degree of solid metal reduction. The role of this electron-shuttling component in enhancing the insoluble metal oxide reduction was further supported by the results of phenotypic studies using pyomelanin overproducing strain. Δ*hmgA* demonstrated a superior HFO reduction capacity to both *S. oneidensis* MR-1 wild-type and Δ*melA* strains with H_2 as the electron donor. With lactate as the electron donor, Δ*hmgA* and *S. oneidensis* MR-1 demonstrated superior HFO reduction capacity compared with Δ*melA*. Notably, the difference between Δ*hmgA* and the wild-type Fe (III) reduction rates was substantially smaller when lactate was used as the electron donor. While this may be attributed to differences in starting cell densities used for H_2- (10^8 cells mL^{-1}) and lactate- (10^7 cells mL^{-1}) driven assays, the results may also reflect the organization of the electron transport chain in *S. oneidensis* MR-1. Earlier studies of metal reduction in different *Shewanella* have shown distinct electron donor dependency with faster rates observed for H_2 than for lactate (Liu *et al.*, 2002). It was proposed that hydrogenase-directed ET provides a more direct path to terminal reductases, while electrons released from lactate dehydrogenase have to travel more circuitous routes. Alternatively, the small size and neutral charge of H_2 may allow for faster diffusion rates and less energy requirement to migrate to sites of enzymatic activity (Liu *et al.*, 2002).

The genetic and physiological evidence of enhanced ET conferred to the cell surface by pyomelanin was further extended using electrochemical analysis. We were able to identify specific surface-associated redox couples through CV and demonstrate the contribution of pyomelanin to enhanced ET at the cell surface. It should be noted that the faster scan rates used here may decrease the resolution of CVs compared with lower scan rates. Lower scan rates are ideal for monitoring growing biofilms (Marsili *et al.*, 2008). The higher scan rates used here were necessary in order to prevent physiological changes from occurring during analysis. While higher scan rates may decrease the resolution of specific redox couples, this approach allowed for differentiation of redox couples between strains.

The increase in $E^{\circ\prime}$ of Δ*melA* grown in the presence of pyomelanin (estimated to be the same concentration of pyomelanin produced by *S. oneidensis* MR-1) essentially restored the $E^{\circ\prime}$ of this strain to that of *S. oneidensis* MR-1 and the more negative redox couple of Δ*hmgA*. This provided strong evidence that existing ET mechanisms were enhanced through surface complexation of pyomelanin.

Our data from cell suspensions and pyomelanin–riboflavin solutions suggest that one of the redox couples is that of riboflavin. Soluble riboflavin was not detected in the supernatant fluids from electrochemistry studies and thus was likely associated with pyomelanin on the cell surface. Riboflavin immobilization (Pereira *et al.*, 2003) as well as enhanced electrochemical activity of riboflavin by other organic compounds (Shigehara *et al.*, 1981) has been demonstrated, and it likely accounts for the increased peak current of riboflavin in the presence of pyomelanin. While production of riboflavin as a soluble electron shuttle is thermodynamically feasible (Marsili *et al.*, 2008), riboflavin retention by pyomelanin offers a more thermodynamically advantageous scenario. In this case, the retained riboflavin could be recycled as an electron shuttle. Incorporation of riboflavin in the extracellular matrix of Δ*melA* was not detected, indicating that pyomelanin plays a unique role in riboflavin retention. The formal potential of the redox couple depicted in Fig. 4b (Δ*melA*) does not match with that of riboflavin, which is indicative of a thermodynamic difference. The second redox couple, evident after background subtraction, was unexpected but was consistent with

that of cytochromes of various strains of *Shewanella* sp. described previously (Kim *et al.*, 2002). While melanin pigments have been shown to interact with cytochromes (Gan *et al.*, 1976), the identity of this couple at this time is unclear.

The redox couple at about +500 mV vs. Ag(RE), barely detectable in the CV of *S. oneidensis* MR-1, was obvious from the CVs of pyomelanin overproducer Δ*hmgA*, and background subtractions of *S. oneidensis* MR-1 and pyomelanin-supplemented cultures of Δ*melA* can be attributed to pyomelanin, based on the CVs of concentrated pyomelanin and the absence of such a redox couple from Δ*melA*. Peak-to-peak separation of oxidation and reduction waves in Figs 4d and 7a allowed for the calculation of apparent rate constants via Laviron's theory (Finklea, 2001; Laviron, 1983). The apparent rate constant (k°) values obtained were $4.0 \times 10^{-6}\,s^{-1}$ for Δ*hmgA* and $2.1 \times 10^{-4}\,s^{-1}$ for 10 mg pyomelanin in 90 mg carbon paste. The difference in redox couples between the pyomelanin from cell suspensions and two concentrations of pyomelanin alone may be a result of the amount of pyomelanin in each study. Limitations of the ET rate because of film thickness have also been demonstrated in other studies (Oyama & Anson, 1980; Shigehara *et al.*, 1981; Vinodgopal *et al.*, 2004). Other plausible factors contributing to differences in the electrochemical behavior of pyomelanin include the degree of hydration or how pyomelanin is incorporated onto the cell surface, especially in relation to the potential insulating properties of exopolysaccharides (Finkenstadt, 2005).

Environmental concentrations of tyrosine or phenylalanine are expected to promote pyomelanin production in *Shewanella*, and thus contribute to increased physiological activity and biogeochemical cycling of metals. The environmental tyrosine concentrations reported (Martens & Loeffelmann, 2003; McLain & Martens, 2005) would be sufficient to produce enough pyomelanin to accelerate metal reduction rates by *S. oneidensis* in the subsurface or sediments, based on previous studies (Turick *et al.*, 2002). Other habitats of *Shewanella* include associations with humans as opportunistic pathogens, algae (Venkateswaran *et al.*, 1999) and biofilms where pyomelanin precursors are likely present in sufficient supply. Our evidence for pyomelanin production from prolonged incubation suggests that lysed cells in high concentration could provide enough amino acid precursors for pyomelanin production. The low concentration of pyomelanin associated with *S. oneidensis* MR-1 from prolonged growth in LBSM was enough to increase HFO reduction by about 10% and corroborated previous work (Turick *et al.*, 2002). This scenario is likely to occur in the environment, especially in biofilms, and could also contribute to accelerated ET. Furthermore, the *melA* gene is upregulated in *S. oneidensis* during growth in aerobic biofilms (McLean *et al.*, 2008), suggesting that pyomelanin may play an important role under these conditions. Similarly, pyomelanin-producing strains of *Pseudomonas aeruginosa* were more evident in biofilms compared with planktonic cells (Boles *et al.*, 2004), further indicating that pyomelanin production is part of a survival strategy in biofilms.

In the present study, cells were grown aerobically for pyomelanin production to proceed, and then analyzed under anaerobic conditions for Fe(III) oxide reduction. This switch from oxic to anoxic growth conditions is consistent with the environmental conditions encountered by *S. oneidensis* MR-1, an organism associated with carbon-rich eutrophic environments that span from anoxic to highly oxygenated zones. Occupying chemically and redox-stratified niches requires the ability to adjust rapidly to changes in electron donor/acceptor type and availability. The ability of *Shewanella* to thrive in such dynamic environments must ultimately be reflected in the flexibility of energy-generating and central carbon metabolic pathways. In that regard, pyomelanin production during periods of decreasing oxygen concentration and its subsequent utilization as a terminal electron acceptor and electron shuttle during respiration of solid phase Fe(III) oxides (Turick *et al.*, 2002) could provide a competitive advantage to the *Shewanella* species and contribute to accelerated biogeochemical cycling of metals.

Acknowledgements

The authors thank Sterling Tommellini for assistance with HPCE and Thomas H. Cromartie of Zenica Agrichemicals for furnishing the sulcotrione. This research was supported in part through funding by the Department of Energy (DOE) Office of Science NABIR/ERSP and Genomics: GTL programs, the Savannah River National Laboratory Directed Research and Development Program, and Soil and Groundwater Closure Projects of the Savannah River Site funded through DOE-Environmental Management Program. Battelle Memorial Institute operates PNNL for the DOE under contract DE-AC05-76RL01830. This document was prepared in conjunction with work accomplished at SRNL under Contract No. DE-AC09-08SR22470 with the US Department of Energy.

References

Bard AJ, Parson R & Jordan J (1985) *Standard Potentials in Aqueous Solution*. Marcel Dekker Inc., NY.

Blomfield IC, Vaughn V, Rest RF & Eisenstein BI (1991) Allelic exchange in *Escherichia coli* using the *Bacillus subtilis sacB* gene and a temperature-sensitive pSC101 replicon. *Mol Microbiol* **5**: 1447–1457.

Boles BR, Thoendel M & Singh PK (2004) Self-generated diversity produces "insurance effects" in biofilm communities. *P Nat Acad Sci USA* **101**: 16630–16635.

Chatfield CH & Cianciotto NP (2007) The secreted pyomelanin pigment of *Legionella pneumophila* confers ferric reductase activity. *Infect Immun* **75**: 4062–4070.

Coon SL, Kotob S, Jarvis BB, Wang S, Fuqua WC & Weiner RM (1994) Homogentisic acid is the product of MelA, which mediated melanogenesis in the marine bacterium *Shewanella colwelliana* D. *Appl Environ Microb* **60**: 3006–3010.

Dadachova E, Bryan RA, Huang X, Moadel T, Schweitzer AD, Aisen P, Nosanchuk JD & Casadevall A (2007) Ionizing radiation changes the electronic properties of melanin and enhances the growth of melanized fungi. *PLoS ONE* **5**: e457.

David C, Daro A, Szalai E, Atarhouch T & Mergeay M (1996) Formation of polymeric pigments in the presence of bacteria and comparison with chemical oxidative coupling-II. Catabolism of tyrosine and hydroxyphenylacetic acid by *Alcaligenes eutrophus* CH34 and mutants. *Eur Polym J* **32**: 669–697.

Dehio C & Meyer M (1997) Maintenance of broad-host-range incompatibility group P and group Q plasmids and transposition of *Tn*5 in *Bartonella henselae* following conjugal plasmid transfer from *Escherichia coli*. *J Bacteriol* **179**: 538–540.

de Lorenzo V, Herrero M, Jakubzik U & Timmis K (1990) Mini-Tn5 transposon derivatives for insertion mutagenesis, promoter probing, and chromosomal insertion of cloned DNA in Gram-negative eubacteria. *J Bacteriol* **172**: 6568–6572.

Ellis DH & Griffiths DA (1974) The location and analysis of melanins in cell walls of some soil fungi. *Can J Microbiol* **20**: 1379–1386.

Fellman JH, Fujita TS & Roth ES (1972) Assay, properties and tissue distribution of *p*-hydroxyphenylpyruvate hydroxylase. *Biochim Biophys Acta* **284**: 90–100.

Finkenstadt VL (2005) Natural polysaccharides as electroactive polymers. *Appl Microbiol Biot* **67**: 735–745.

Finklea HO (2001) Theory of coupled electron-proton transfer with potential-dependent transfer coefficients for redox couples attached to electrodes. *J Phys Chem B* **105**: 8685–8693.

Fuqua WC & Weiner RM (1993) The *melA* gene is essential for melanin production in the marine bacterium *Shewanella colwelliana*. *J Gen Microbiol* **139**: 1105–1114.

Gan EV, Haberman HF & Menon IA (1976) Electron transfer properties of melanin. *Arch Biochem Biophys* **173**: 666–672.

Gorby YA, Yanina S, McLean JS *et al.* (2006) Electrically conductive bacterial nanowires produced by *Shewanella oneidensis* strain MR-1 and other microorganisms. *P Nat Acad Sci USA* **103**: 11358–11363.

Ho SN, Hunt HD, Horton RM, Pullen JK & Pease LR (1989) Site-directed mutagenesis by overlap extension using the polymerase chain reaction. *Gene* **77**: 51–59.

Hobbie JE, Daley RJ & Jasper S (1977) Use of Nucleopore filters for counting bacteria by fluorescence microscopy. *Appl Environ Microb* **33**: 1225–1228.

Kim HJ, Park HS, Hyun MS, Chang IS, Kim M & Kim BH (2002) A mediator-less microbial fuel cell using a metal reducing bacterium, *Shewanella putrefaciens*. *Enzyme Microb Tech* **30**: 145–152.

Kotob SI, Coon SL, Quintero EJ & Weiner RM (1995) Homogentisic acid is the primary precursor of melanin synthesis in *Vibrio cholera*, a *Hyphomonas* strain, and *Shewanella colwelliana*. *Appl Environ Microb* **61**: 1620–1622.

Laviron E (1983) Electrochemical reactions with protonations at equilibrium: part VIII. The 2 e, $2H^+$ reaction (nine-member square scheme) for a surface or for a heterogeneous reaction in the absence of disproportionation and dimerization reactions. *J Electroanal Chem* **146**: 15–36.

Lee DL, Prisbylla MP, Cromartie TH, Dargin DP, Howard SW, Provan WM, Ellis MK, Fraser T & Mutter LC (1997) The discovery and structural requirements of inhibitors of *p*-hydroxyphenylpyruvate dioxygenase. *Weed Sci* **45**: 601–609.

Lehninger AL (1975) Oxidative degradation of amino acids. *Biochemistry*, pp. 568–570. Worth Publishers, New York, NY.

Lindblad B, Lindstedt G, Lindstedt S & Rundgren M (1977) Purification and some properties of human 4-hydroxyphenylpyruvate dioxygenase. *J Biol Chem* **252**: 5073–5084.

Link A, Phillips JD & Church GM (1997) Methods for generating precise deletions and insertions in the genome of wild-type *Escherichia coli*: application to open reading frame characterization. *J Bacteriol* **179**: 6228–6237.

Liu C, Gorby Y, Zachara JM, Fredrickson JK & Brown CF (2002) Reduction kinetics of Fe (III), Co (III), U (VI), Cr (VI), and Tc (VII) in cultures of dissimilatory metal-reducing bacteria. *Biotechnol Bioeng* **80**: 637–649.

Lloyd JR (2003) Microbial reduction of metals and radionuclides. *FEMS Microbiol Rev* **27**: 411–425.

Marsili E, Baron DB, Shikhare ID, Coursolle D, Gralnick JA & Bond DR (2008) *Shewanella* secretes flavins that mediate extracellular electron transfer. *P Nat Acad Sci USA* **105**: 3968–3973.

Martens DA & Loeffelmann KL (2003) Soil amino acid composition quantified by acid hydrolysis and anion chromatography-pulsed amperometry. *J Agr Food Chem* **51**: 6521–6529.

McCuen PJ (1988) Culture media components. *Manual of BBL Products and Laboratory Procedures* (Power DA, ed), pp. 293–294. Beckton Dickinson Systems, Cockeysville, MD.

McLain JET & Martens DA (2005) Nitrous oxide flux from soil amino acid mineralization. *Soil Biol Biochem* **37**: 289–299.

McLean J, Purvis OW, Williamson BJ & Bailey EH (1998) Role for lichen melanins in uranium remediation. *Nature* **391**: 649–650.

McLean JS, Pinchuk GE, Geydebredkht OV *et al.* (2008) Oxygen-dependent autoaggregation in *Shewanella oneidensis* MR-1. *Environ Microbiol* **10**: 1861–1876.

Oyama N & Anson FC (1980) Catalysis of electrode processes by multiply-charged metal complexes electrostatically bound to polyelectrolyte coatings on graphite electrodes, and the use of

polymer-coated rotating disk electrodes in diagnosing kinetic and conduction mechanisms. *Anal Chem* **52**: 1192–1198.

Paz MA, Fluckiger RA, Boak A, Kagan HM & Gallop PM (1991) Specific detection of quinoproteins by redox-cycling staining. *J Biol Chem* **266**: 689–692.

Pereira AC, Santos de SA & Kubota LT (2003) Electrochemical behavior of riboflavin immobilized on different matrices. *J Colloid Interf Sci* **265**: 351–358.

Prota G (1992) Natural and synthetic melanins. *Melanins and Melanogenesis* (Prota G, ed), pp. 63–87. Academic Press Inc., San Diego, CA.

Ruzafa C, Solano F & Sanchez-Amat A (1994) The protein encoded by the *Shewanella colwelliana melA* gene is *p*-hydroxyphenylpyruvate dioxygenase. *FEMS Microbiol Lett* **124**: 179–184.

Ruzafa C, Sanchez-Amat A & Solano F (1995) Characterization of the melanogenic system in *Vibrio cholerae* ATCC 14035. *Pigm Cell Res* **8**: 147–152.

Saltikov CW, Cifuentes A, Venkateswaran K & Newman DK (2003) The *ars* detoxification system is advantageous but not required for As(V) respiration by the genetically tractable *Shewanella* species strain ANA-3. *Appl Environ Microb* **69**: 2800–2809.

Sanchez-Amat A, Ruzafa C & Solano F (1998) Comparative tyrosine degradation in *Vibrio cholerae* strains. The strain ATCC 14035 as a prokaryotic melanogenic model of homogentisate-releasing cell. *Comp Biochem Phys B* **119**: 557–562.

Schulz A, Ort O, Beyer P & Kleninig H (1993) SC-0051, a 2-benzoyl-cyclohexane-1,3-dione bleaching herbicide, is a potent inhibitor of the enzyme *p*-hydroxyphenylpyruvate dioxygenase. *FEBS Lett* **318**: 162–166.

Secor J (1994) Inhibition of barnygrass 4-hydroxyphenylpyruvate dioxygenase by sulcotrione. *Plant Physiol* **106**: 1429–1433.

Serpentini C-L, Gauchet C, de Montauzon D, Comtat M, Ginestar J & Paillous N (2000) First electrochemical investigation of redox properties of DOPA-melanins by means of carbon paste electrode. *Electrochim ACTA* **45**: 1663–1668.

Shigehara K, Oyama N & Anson FC (1981) Electrochemical responses of electrodes coated with redox polymers. Evidence for control of charge-transfer rates across polymeric layers by electron exchange between incorporated redox sites. *J Am Chem Soc* **103**: 2552–2558.

Steinert M, Engelhard H, Flügel M, Wintermeyer E & Hacker J (1995) The Lly protein protects *Legionella pneumophila* from light but does not directly influence its intracellular survival in *Hartmannella vermiformis*. *Appl Environ Microb* **61**: 2428–2430.

Turick CE, Tisa LS & Caccavo F Jr (2002) Melanin production and use as a soluble electron shuttle for Fe(III) oxide reduction and as a terminal electron acceptor by *Shewanella algae* BrY. *Appl Environ Microb* **68**: 2436–2444.

Turick CE, Caccavo F Jr & Tisa LS (2003) Electron transfer from *Shewanella algae* BrY to hydrous ferric oxide is mediated by cell-associated melanin. *FEMS Microbiol Lett* **220**: 99–104.

Turick CE, Caccavo F Jr & Tisa LS (2008a) Pyomelanin is produced by *Shewanella algae* BrY and affected by exogenous iron. *Can J Microbiol* **54**: 334–339.

Turick CE, Knox AS, Leverette CL & Kritzas YG (2008b) *In-situ* uranium stabilization by microbial metabolites. *J Environ Radioactiv* **99**: 890–899.

Venkateswaran K, Moser DP, Dollhopf ME *et al.* (1999) Polyphasic taxonomy of the genus *Shewanella* and description of *Shewanella oneidensis* sp. nov. Internat. *J Syst Bacteriol* **49**: 705–724.

Vinodgopal K, Subramanian V & Kamat PV (2004) Selective electrochemical detection of ionic and neutral species using films of Suwannee River humic acid. *Environ Sci Technol* **38**: 2161–2166.

Waite JH & Benedict CV (1984) Assay of dihydroxyphenylalanine (Dopa) in invertebrate structural proteins. *Meth Enzymol* **107**: 397–413.

Wan XF, VerBerkmoes NC, McCue LA *et al.* (2004) Transcriptomic and proteomic characterization of the Fur modulon in the metal-reducing bacterium *Shewanella oneidensis*. *J Bacteriol* **186**: 8385–8400.

Yabuuchi E & Omyama A (1972) Characterization of "pyomelanin"-producing strains of *Pseudomonas aeruginosa*. *Int J Syst Bacteriol* **22**: 53–64.

Zughaier SM, Ryley HC & Jackson SK (1999) A melanin pigment purified from an epidemic strain of *Burkholderia cepacia* attenuates monocyte respiratory burst activity by scavenging superoxide anion. *Infect Immun* **67**: 908–913.